MRS Internet Journal of Nitride Semiconductor Research

*Volume 2, Article 23*

# XPS study of Au/GaN and Pt/GaN contacts

R. Sporken, C. Silien, F. Malengreau, K. Grigorov, R. Caudano
Facultés Universitaires Notre-Dame de la Paix , Belgium

F. J. Sánchez, E. Calleja, E. Muñoz
Dpt. Ingeniería Electrónica, E.T.S.I. Telecomunicación, Politécnica, Ciudad Universitaria

B. Beaumont, Pierre Gibart
Centre de Recherche sur l'Hetero-Epitaxie et ses Applications, CRHEA-CNRS

This article was received on June 10, 1997 and accepted on September 4, 1997.

## Abstract

Au/GaN and Pt/GaN contacts have been studied with XPS. According to XPS depth profiling, the N signal is weak in the region below the metal contact and the Pt or Au signal decreases much more slowly than expected for a sharp interface. Next, we have performed in situ studies of the formation of Au contacts on GaN. In contrast to the results from depth profiling, we observe 2D growth and little or no chemical interaction between Au and GaN. This suggests that conventional calculations of sputtering yields and ion-beam-induced mixing cannot be applied to the analysis of noble metal/GaN depth profiles. Heating during or after Au deposition results in strong clustering, observed by both XPS and AFM. The Schottky barrier height measured by XPS is 1.15 eV.

## 1. Introduction

GaN has attracted considerable interest in recent years because of its wide range of applications, including blue/ultra-violet light emitting devices, ultra-violet detectors and high power/high temperature electronics. These applications are possible because of the large direct band gap of GaN (3.4 eV), and because of its remarkable stability in aggressive environments.

In this context, it is important to study the properties of metal-GaN contacts, because one must be able to produce stable metal contacts with well-defined electrical properties. In this work, Schottky contacts of Pt and Au on GaN were studied by XPS. In the first part of this paper, we describe the study of such contacts by depth profiling with x-ray photoelectron spectroscopy (XPS). This technique is destructive and can introduce several artefacts due to the use of an energetic ion beam to sputter through the metal layer. Therefore, in the second part of the paper, a detailed in situ study by XPS of the formation of Au/GaN interfaces is described. Finally, we have investigated the effect of thermal annealing on the structure of the Au/GaN interface, and have found that Au has a strong tendency to form large clusters on GaN at elevated temperature.

## 2. Experimental

The GaN samples are epitaxial films of GaN grown on (0001) sapphire substrates by metalorganic vapor phase epitaxy (MOVPE) at atmospheric pressure. All samples are n-type, with carrier concentration in the $10^{17}$ - $10^{18}$ $cm^{-3}$ range. Details about the growth of such layers are published elsewhere [1]. For the study of metal-GaN by XPS depth profiles, the samples were transferred into a metallization chamber where a 150 nm thick layer of Pt or Au was deposited using an electron gun evaporator, without intentionally heating the samples. It should be noted that samples had to be exposed to atmosphere between growth of GaN and metallization.

For the in-situ studies of the formation of metal/GaN interfaces, the GaN samples were transferred through air

https://doi.org/10.1557/S1092578300001496 Published online by Cambridge University Press

into the XPS system. Various surface treatments were applied to the surface prior to metallization; they will be described in the results section as needed. Au was then evaporated from a Knudsen cell at a rate of about 0.1 nm/s, calibrated using a quartz crystal monitor and corrected for distance from the Au evaporator assuming $r^{-2}$ dependence. Au coverage will be indicated in atoms/$cm^2$. In the case of a uniform Au layer, 5.6 $10^{15}$ $cm^{-2}$ corresponds to a thickness of 1 nm. Metallization was interrupted several times to record XPS spectra. The samples were transferred between the metallization chamber and the XPS analysis chamber through ultra-high vacuum.

XPS measurements were performed with an SSX-100 spectrometer from Surface Science Instruments. This instrument uses a monochromatic and focused x-ray source (Al $K_{\alpha}$, $h\nu$ = 1486.6 eV) and a hemispherical analyzer. For the measurements presented here, a spot size of 0.6 mm diameter was used. All binding energies are relative to the Fermi level. Calibration was achieved by measuring spectra of both the Fermi edge and the Au 4f core levels on a thick layer of Au on the Ta sample holder. XPS depth profiles were recorded by alternating sputtering with Ar ions and XPS measurements. A differentially pumped ion gun (Leybold Instruments) was used to produce the 4 keV ion beam. The ion beam was rastered over an area of 2x3 $mm^2$ which had to be carefully aligned with the sample because they are of approximately the same size. The sputter rate, determined using a $SiO_2$/Si reference sample, was 3.3 $10^{-2}$ nm/s.

# 3. Results

## 3.1. XPS depth profiles

XPS depth profiles were recorded on Pt/GaN and Au/GaN contacts. Pt 4f or Au 4f, Ga 3d, N 1s, C 1s and O 1s core level spectra were measured. Since the results for Au and Pt are very similar, only those for Pt/GaN contacts will be described here. With increasing sputter time, the Pt signal decreases, but even after an equivalent thickness of 220 nm has been removed, some Pt is still detected, although the nominal thickness of the Pt layer was 150 nm. Another striking feature of the spectra is a second Pt 4f component which is seen in the spectra after removing 132 nm or more. Figure 1 shows how the Pt 4f spectrum can be fitted to the sum of a two spin-orbit doublets and a Shirley-type background. The line shape of the doublet at lower binding energy is a Doniach-Sunjic function broadened with a Gaussian; this is characteristic of metallic Pt. The doublet at higher binding energy is a Voigt function and would normally be attributed to Pt in a different chemical environment. Because of the small value of the spin-orbit splitting in the Ga 3d spectra, no attempt was made to perform a detailed line shape analysis of these peaks. The peak area was obtained by numerical integration after subtracting a suitable background. The same procedure was applied to the C 1s and O 1s spectra. For the N 1s level, the procedure is somewhat more complicated because this peak overlaps with Ga Auger transitions. The determination of the N 1s peak area is illustrated in figure 2. First, a horizontal background was adjusted on the high binding energy side of the spectra. A Voigt-shaped peak was then fitted by minimizing $\chi^2$ over the energy range where the Ga Auger signal is weak. The integral of this Voigt function is then taken as the N 1s peak area. The validity of this approach was tested on a GaN sample without a metal layer. The sample was first sputtered with Argon ions for about 2 minutes to remove surface contamination. The N 1s and Ga 3d peak areas were then determined as described before and converted into atomic concentration using the following sensitivity factors:

$$S = S_{Scofield} E_k^{0.7} \quad , \qquad (1)$$

where $S_{Scofield}$ is the Scofield sensitivity factor [2] and $E_k$ is the kinetic energy of the photoelectrons. The result is $C_{Ga} = 0.52 \pm 0.03$ and $C_N = 0.48 \pm 0.03$. Here, $C_{Ga}$ and $C_N$ are atomic concentrations of Ga and N. We conclude that the fitting procedure for N 1s and the sensitivity factors can be applied to determine atomic concentrations for Ga and N from our XPS spectra.

The same procedure was then applied to the entire depth profile data. For Pt, the two Pt 4f doublets, determined by peak fitting, were treated separately. For O and C, peak areas were obtained by numerical integration of the spectra, after subtracting a linear background. Finally, atomic concentrations were calculated using sensitivity factors from equation 1. A typical depth profile is shown in figure 3. Several observations can be made from this depth profile. O and C signals are very low, except at the surface (not shown). In some cases, there seems to be a very small O signal near the Pt/GaN interface, but this may not be significant. The Pt/GaN interface is reached after sputtering the equivalent of slightly more than 100 nm, which is reasonably close to the nominal thickness of the Pt layer. The Ga:N ratio is very different from the expected 1:1 ratio below the metal layer. In order to check if this can be explained by differential sputtering, we have calculated the sputtering yield for Ga and N. For our experimental conditions, a calculation using the TRIM program [3] gives a

https://doi.org/10.1557/S1092578300001496 Published online by Cambridge University Press

difference in sputtering yield between Ga and N of less than 5 %, the yield for N being slightly higher. If this calculation is valid for our GaN layers, it would suggest that the deviation from a 1:1 stoechiometry cannot be explained by differential sputtering alone.

The decrease of the Pt signal is compared with a calculation for an abrupt interface. This calculation follows the method described by Seah and Hunt [4]. We use an effective electron escape depth of 2.5 nm and a projected range z* of the film atoms into the substrate of 8 nm. Calculations using TRIM [3] or based on the LSS theory [5] give z* = 4.4 and 7 nm respectively for 4 keV Ar atoms in GaN, and the range for Pt should be less because only a fraction of the energy is transferred from Ar to Pt. However, even with z* = 8 nm, the measured profile is much more diffuse than the calculated one. Good agreement is obtained for z* = 16 nm, but this value is unrealistically high. The same holds for Au/GaN contacts, where z* = 16 nm is also needed to fit the experimental data. More work was thus needed in order to determine if the difference between experiment and calculation is due to the structure of the interface or if it is related to other artifacts induced by the ion beam. Therefore, we studied the formation of Au/GaN interfaces *in situ*. This is the topic of the next section.

## 3.2. In-situ study of Au/GaN interface formation

First, we have compared several methods for preparing GaN substrates after exposure to air, prior to metallization. Figure 4 shows XPS survey spectra obtained on three GaN samples. Sample #1 was simply cleaned in organic solvents, sample #2 was chemically cleaned using hot KOH and aqua regia, and sample #3 was treated like sample #2 and then heated in UHV to 900°C. Sample #1 is heavily contaminated with O and C, and the Ga:N atomic concentration ratio is 1.6. Sample #2 has about half the C contamination of sample #1, but there is a small Cl contamination. The Ga:N ratio is much closer to 1 (1.2). Heating the sample to 900°C removes the Cl and O contamination. A small amount of C is still present on the surface. The Ga:N ratio is the same as for sample #2. Since sample #3 has the cleanest surface of the three samples studied here, the formation of the Au/GaN interface has been studied in detail on this sample. We shall describe these results below; the difference with other samples will be described in more detail in a future publication. Figure 5 shows some typical Au 4f spectra obtained at various stages of the deposition of Au on GaN sample #3. These spectra have been fitted with up to three spin-orbit doublets, which will be labeled i, m and m' hereafter. Although some of these doublets are not immediately visible on the raw data, more than one doublet has to be included to produce satisfactory results by peak fitting. The results from peak fitting presented here are based on numerous tests, including examination of the residuals and checks for consistency among many spectra from several samples. For each spectrum, we used the lowest number of doublets required to produce a good fit. For doublet m, a Doniach-Sunjic lineshape was used, with the spin-orbit parameters and the singularity index fixed at the values obtained for a thick layer of Au ($\Delta_{s-o}$ = 3.67 eV, I ($4f_{7/2}$) / I ($4f_{5/2}$) = 0.75, $\alpha$ =0.064). These values are consistent with published data [6]. The lineshape of the other doublets is a mixed Gaussian-Lorentzian curve. Finally, the whole spectrum is broadened with a Gaussian of 0.75 ± 0.05 eV full-width at half-maximum (FWHM), except for the very early stages where a broadening of 1 eV is used. The intensity of these three components versus Au coverage is shown in Figure 6. Obviously, doublet m is by far the strongest at all stages of the interface formation. Its binding energy (maximum of the $4f_{7/2}$ peak) stabilizes at 84 eV when Au coverage exceeds $10^{16}$ $cm^{-2}$. This corresponds to metallic Au. Doublet i appears only at the early stages of the interface formation and has a weak maximum near 5 $10^{15}$ $cm^{-2}$. The corresponding binding energy is roughly 0.7 eV above the metal peak. This is assigned to an interface peak. Since the starting surface is Ga-rich (see above), we suggest that this peak is characteristic of Au-Ga bonds at the Au/GaN interface. The low intensity of this interface peak suggests that it corresponds to one atomic plane only and that there is no reaction or intermixing at the Au/GaN interface. Finally, doublet m', at a binding energy somewhat lower than that of metallic Au, appears only at larger Au coverage. The origin of this weak doublet will be discussed later. The total Au 4f intensity was fitted by the following relation:

$$I(d) = I_0 \, [1-\exp(-d/\lambda\cos\theta)], \quad (2)$$

where $I_0$ and $\lambda$ are fitting parameters, and $\theta$ is the angle between the lens axis and the normal to the surface (55° in our case). $\lambda$ is the escape depth of the photoelectrons; the best fit is obtained for $\lambda$ = 4 nm. This suggests layer-by-layer growth of Au on GaN.

The decrease of the Ga 3d and N 1s signals confirms this growth mode (Figure 7). The signal intensities were obtained in the same way as for the analysis of XPS depth profiles described before. An exponential decay was fitted to the data; the best fit is obtained with $\lambda$ = 4.1 nm and 3.3 nm for Ga 3d and N 1s respectively. The values of the electron escape depth are of the order of magnitude which would be expected for photoelectrons in XPS. However, these values should not be considered as a quantitative measure of $\lambda$, because they rely on

https://doi.org/10.1557/S1092578300001496 Published online by Cambridge University Press

the thickness calibration using the quartz monitor, and they assume unity sticking coefficient of Au on GaN. Nevertheless, the dependence on kinetic energy deduced from our measurements is as expected, since we find $\lambda_{Ga3d} \geq \lambda_{Au4f} > \lambda_{N1s}$ . The Ga 3d peak position is found to increase by about 1 eV during the first stages of the interface formation on sample #3. This position was determined from the half-width point at half-height. The position of the N 1s peak versus Au coverage follows a similar curve. Since we do not observe a significant change in peak shape for either Ga 3d and N 1s lines, we attribute this effect to changes in band bending. The Schottky barrier height can be determined from the XPS data. Indeed, all energies are measured with respect to the Fermi level, which was checked repeatedly during these experiments. Furthermore, the distance between the Ga 3d core level and the valence band maximum was measured on GaN sample #3 prior to Au evaporation. The value is 17.8 eV, in excellent agreement with literature data [7]. Figure 8 shows the position of the Fermi level with respect to the band gap. The starting surface is far from flat-band conditions, since the Fermi level is about 1.2 eV above the valence band maximum, and the carrier concentration of this sample, measured by Hall effect, is n = 1.2 $10^{17}$ $cm^{-3}$, n-type. With increasing Au coverage, band bending changes, and eventually, the Fermi level stabilizes at 1.15 $\pm$ 0.15 eV below the conduction band minimum. Since the conductivity of GaN #3 is n-type, this distance is the Schottky barrier height of the Au/GaN contact. The value of 1.15 $\pm$ 0.15 eV is the same as the result from electrical characterization by Binari et al. [8]; it is also in excellent agreement with the calculated value of 1.05 eV for ideal Au Schottky contacts on $\alpha$-GaN [9]; it is somewhat larger than other values obtained by current-voltage and capacitance-voltage methods, which range from 0.84 to 0.98 eV [10], [11]. Next, we investigated the effect of temperature on the Au/GaN interface. Figure 9 shows Au 4f spectra after annealing sample GaN #3 covered with 10 nm of Au. Compared to the sample before annealing, the area of the Au 4f peak is about two times lower after annealing at 600 °C, about five times lower after annealing at 710 °C, and the peak shape changes drastically. However, the presence of several doublets in the Au 4f spectra is not due to different chemical states, but to differential charging of the sample. This is confirmed most easily in the case of spectrum (b), because the same splitting is observed in the Au 4f spectrum and at the Fermi edge. The binding energy of each of the two doublets in figure 9b with reference to the respective Fermi edge is 84 eV, characteristic of metallic Au. Atomic force microscopy (AFM) images of the surface corresponding to Figure 9b show the presence of large islands covering about 20 % of the surface. The average height of these islands is 25 nm. The XPS and AFM results can be explained if we assume that in addition to the Au islands, there is a thin layer (about 0.5 - 1 nm) of Au between the islands. The doublet at higher apparent binding energy is then due to this thin layer, whereas the other doublet would be from negatively charged Au islands. Also, a very small degree of clustering seems to occur at room temperature, which could explain the presence of the weak doublet m' in the Au 4f spectra in figure 5.

Finally, detailed comparison of the Au/GaN interface formation for the different samples (GaN #1, 2 and 3) will be published elsewhere. The most striking difference is that the growth is not purely layer-by-layer on samples #1 and #2, but gradually changes to island growth. This is found by modeling the XPS intensities of Ga 3d, N 1s and Au 4f versus Au coverage. Also, changes in Au 4f peak shape, similar to the ones observed when Au/GaN is annealed, are observed at higher Au coverage on these samples. This may be due again to electrostatic charging of clusters rather than to chemical shifts.

It is conceivable that clustering of Au on GaN #1 and #2 is due to some extent to the increase in substrate temperature, caused by radiation from the Knudsen cell, because the Au evaporation was interrupted less frequently than for sample #3. However, after 10 minutes in front of the Knudsen cell, the sample temperature stabilizes near 60 °C, which is still low compared to the annealing temperatures which produce a sizable change in the XPS spectra.

## 4. Conclusion

We have studied Au/GaN and Pt/GaN interfaces by XPS. Depth profiling suggests that the interfaces may not be sharp, but in situ studies show no sign of interdiffusion or reaction at the interface at room temperature. A possible explanation for this discrepancy is that the sputtering yield for GaN is much lower than for Pt or Au. This is indeed possible, because most of the ion energy is deposited near the surface in the case of Pt and Au because of the high density of these materials. Therefore, when converting sputter time into depth one should take the change in sputter rate into account. Theoretical simulations of sputtering through the Pt/GaN interface are in progress to clarify this point.

In situ studies show that, at room temperature, Au grows in a layer-by-layer fashion on clean GaN. The Schottky barrier height, calculated from the XPS data, is 1.15 $\pm$ 0.15 eV for Au on n-type GaN. This value is close to the theoretical value for ideal Au/GaN Schottky contacts.

Annealing Au/GaN contacts at 600 °C and above leads to the formation of islands; between these islands, a

https://doi.org/10.1557/S1092578300001496 Published online by Cambridge University Press

thin layer of Au remains. There is still no or very limited interdiffusion at these temperatures. Lower annealing temperatures were not studied. XPS spectra from such samples show at least two Au 4f doublets, corresponding to differential charging of the islands versus the thin layer, rather than different chemical states. This shows that great care must be used when analyzing XPS data from metal/GaN interfaces. On other GaN samples, island formation occurs during the interface formation. The reason could be the different state of the starting surface (these samples had not been heated in UHV), but slightly higher surface temperature during Au evaporation may have affected the growth to some extent.

## Acknowledgments

**We would like to thank F. Wiame for assistance with the AFM measurements. R.S. acknowledges support from the Belgian National Fund for Scientific Research. This work is supported in part by the Belgian Office of Scientific, Technical and Cultural Affairs, and by EU contract ESPRIT-LTR LAQUANI n° 20968.**

## References

[1] B. Beaumont, M. Vaille, T. Boufaden, B. el Jani, P. Gibart, *J. Cryst. Growth* ***170***, 316-320 (1997).

[2]J.H. Scofield, "Hartree-Slater Subshell Photoionization Cross-sections at 1254 and 1487 eV", *J. Electron. Spectrosc. Rel. Phenomena* ***8***, 129 (1976)

[3] J.F. Ziegler, J.P. Biersack, U. Littmark, *The stopping and ranges of ions in solids, Vol. 1* (Pergamon, New York, 1985) .

[4] M. P. Seah, C. P. Hunt, *J. Appl. Phys.* ***56***, 2106 (1984).

[5]J.Lindhard, M.Scharff and H.E.Schiott,"Range concepts and heavy ion ranges", *Mat. Fys. Medd. Dan. Vid. Selsk.* ***33***, 14 (1963)

[6]P.H. Citrin, G.K. Wertheim, Y. Baer, "Surface-atom x-ray photoemission from clean metals: Cu, Ag, and Au", Phys. Rev. **B 27** (6), 3160-3175 (1983)

[7] J. R. Waldrop, R. W. Grant , *Appl. Phys. Lett.* ***68***, 2879-2881 (1996).

[8] S. C. Binari, H. B. Dietrich, G. Kelner, L. B. Rowland, K. Doverspike, D. K. Gaskill, *Electron. Lett.* ***30***, 909-911 (1994).

[9] T. U. Kampen, W. Mönch, *MRS Internet J. Nitride Semicond. Res.* ***1***, 41 (1997).

[10] A.C. Schmitz, A.T. Ping, M. Asif Khan, I. Adesida, *Mater. Res. Soc. Symp. Proc.* ***395***, 831-835 (1996).

[11] P. Hacke, T. Detchprohm, K. Hiramatsu, N. Sawaki , *Appl. Phys. Lett.* ***63***, 2676-2678 (1993).

https://doi.org/10.1557/S1092578300001496 Published online by Cambridge University Press

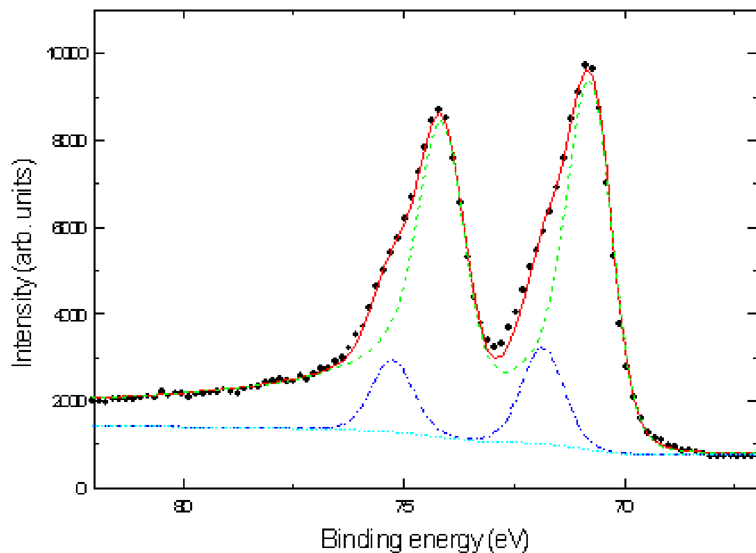


**Figure 1**. Pt 4f core level spectrum recorded after sputtering an equivalent thickness of 134 nm from a nominally 150 nm thick layer of Pt on GaN. The result of least squares peak fitting by two spin-orbit doublets is shown by the dashed and dash-dotted curves (individual doublets) and by the full line (sum of two doublets).

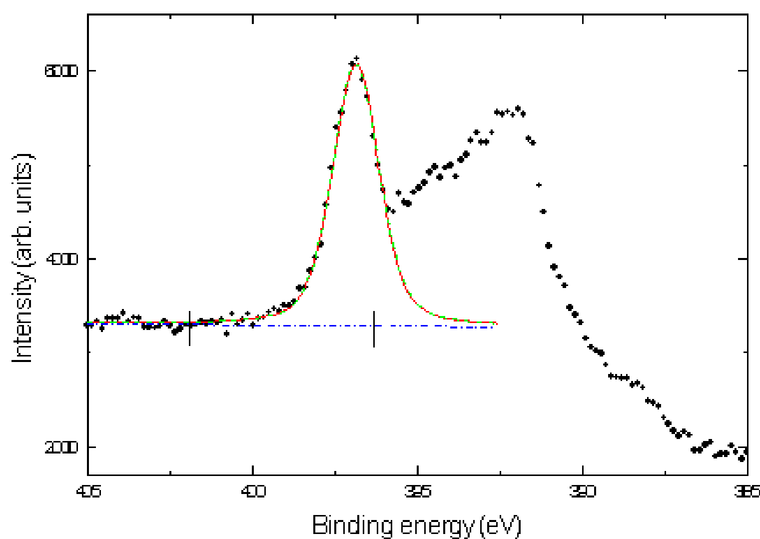


**Figure 2**. N 1s core level spectrum recorded after sputtering an equivalent thickness of 150 nm from a nominally 150 nm thick layer of Pt on GaN. Note the overlap with Ga LMM Auger transitions. Least squares peak fitting was done by minimizing RMS error between data (dots) and fitted curve (line) over the energy interval between the two vertical marks.

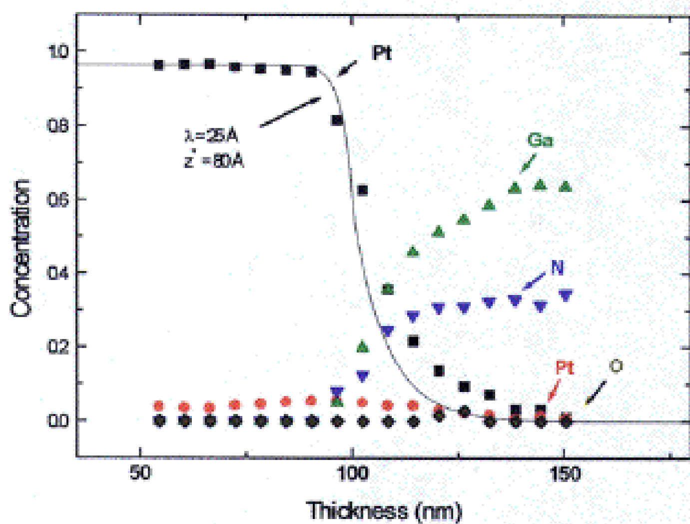


**Figure 3**. Atomic concentration sputter depth profile obtained from XPS data, zoomed around the Pt/GaN interface. Thickness values correspond to equivalent $SiO_2$ thickness. The solid line is a calculated Pt profile, assuming an atomically sharp interface and taking broadening due to electron escape depth and ion beam induced mixing into account. All other sources of broadening are neglected.

https://doi.org/10.1557/S1092578300001496 Published online by Cambridge University Press

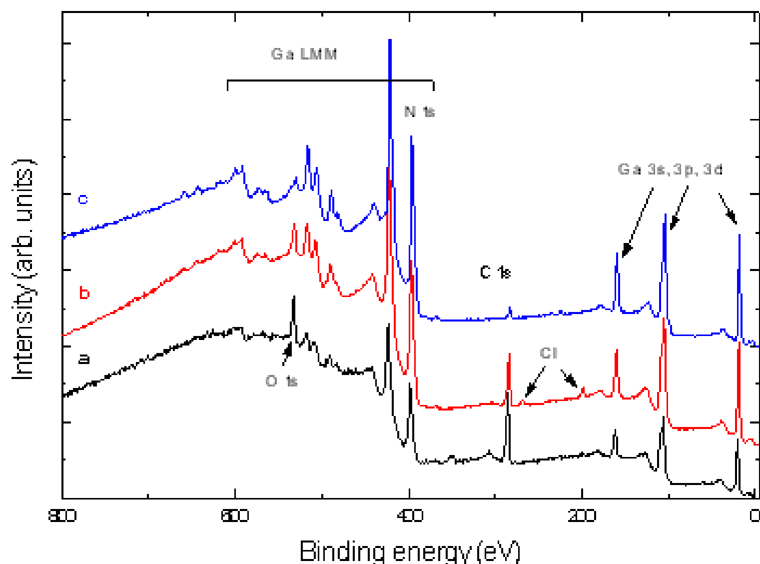


**Figure 4**. XPS survey spectra from GaN on sapphire after different methods of surface preparation: a) sample cleaned in organic solvents; b) cleaned in hot KOH and aqua regia ; c) same as (b) plus heating in UHV at 900 °C.

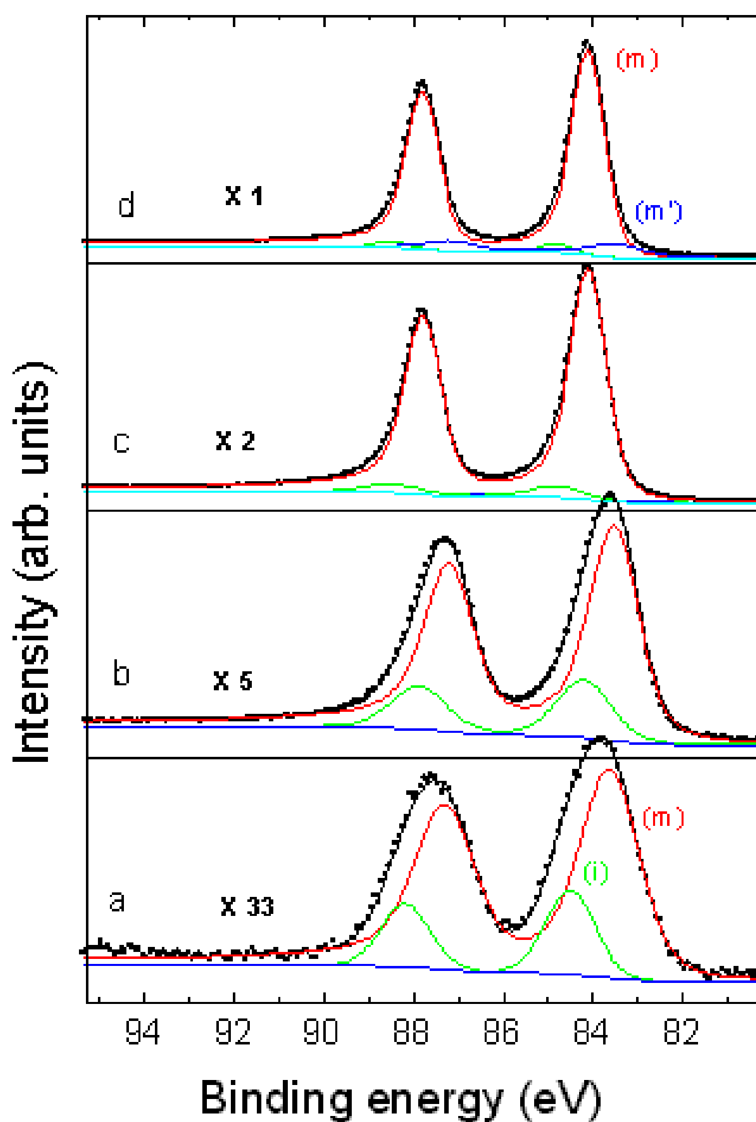


**Figure 5**. Typical Au 4f spectra measured at various stages of the evaporation of Au on GaN #3. The colored lines show the individual doublets used for fitting the spectra, after broadening with a Gaussian. The black line is the resulting calculated spectrum. Au coverage is 5 $10^{14}$ $cm^{-2}$ (a), 5 $10^{15}$ $cm^{-2}$ (b), 1.5 $10^{16}$ $cm^{-2}$ (c), and 5 $10^{16}$ $cm^{-2}$ (d).

https://doi.org/10.1557/S1092578300001496 Published online by Cambridge University Press

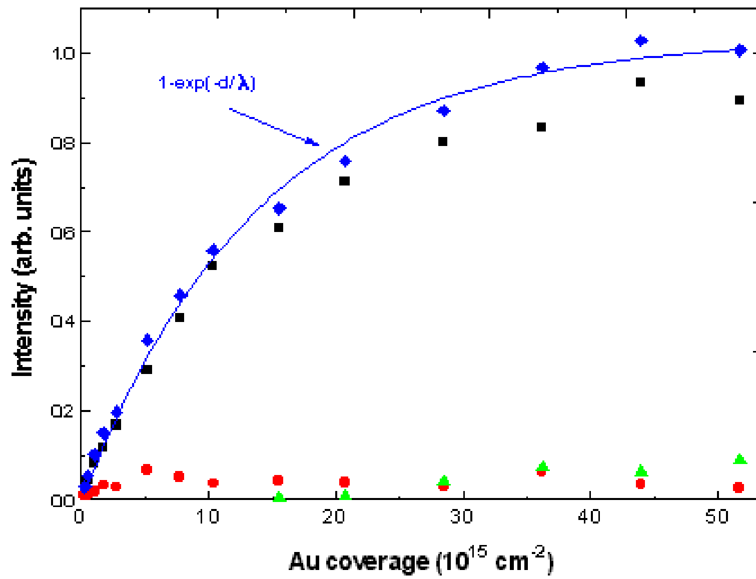


**Figure 6**. Intensity of the Au 4f doublets versus Au thickness on GaN. Blue diamonds correspond to the total Au 4f peak area, while black squares, red circles and green triangles are peak areas for doublets m, i and m', respectively. The blue line is a least-squares fit to the total intensity data, as described in the text.

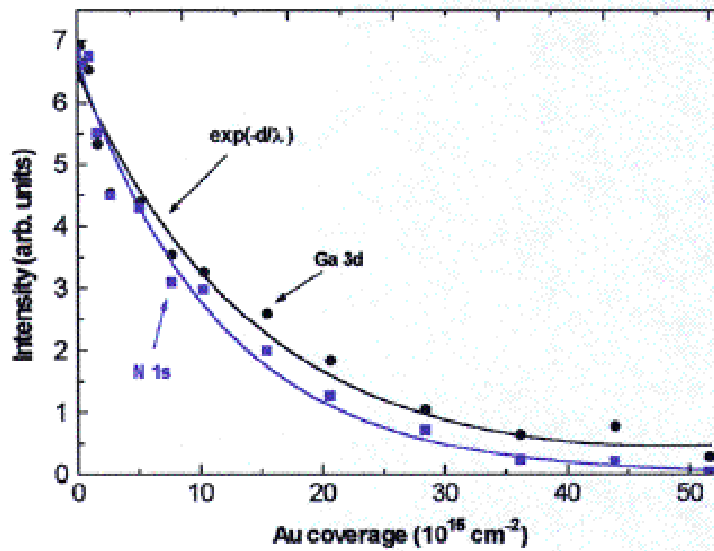


**Figure 7**. Ga 3d and N 1s peak area versus Au coverage. The data have been normalized to the same intensity at low coverage. The lines show the result of an exponential decay fitted to the data.

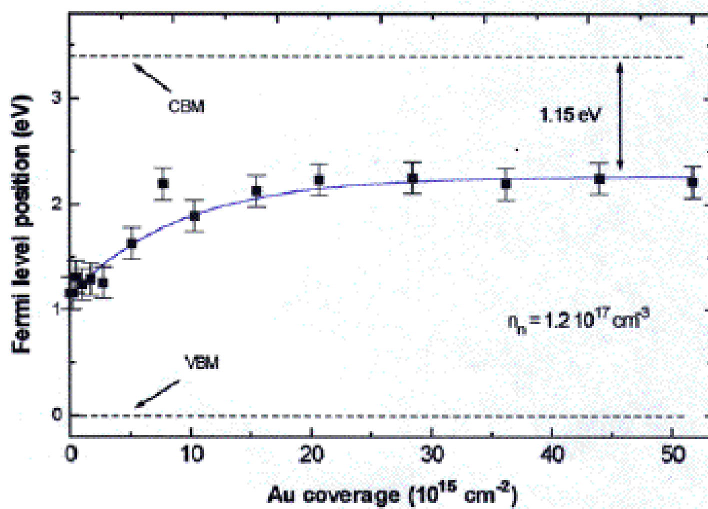


**Figure 8**. Fermi level position within the band gap at the GaN surface as a function of Au coverage.

https://doi.org/10.1557/S1092578300001496 Published online by Cambridge University Press

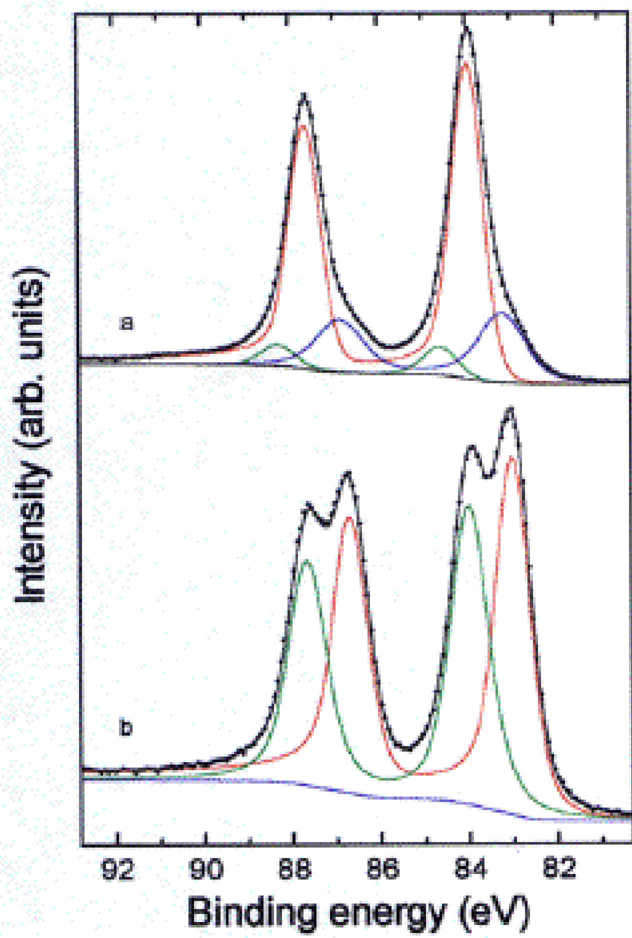


**Figure 9**. Au 4f spectra from sample GaN #3, covered with 5.6 $10^{15}$ $cm^{-2}$ of Au and annealed 6 minutes at 600 °C (a); annealed 21 minutes at 600 °C and 10 minutes at 710 °C.

© 1997 The Materials Research Society



https://doi.org/10.1557/S1092578300001496 Published online by Cambridge University Press